

Enhancing power quality: An Adaline algorithm for direct resonance current extraction in shunt active power filter

Nor Farahaida Abdul Rahman¹, Muhammad Ammirul Atiqi Mohd Zainuri², Naeem M. S. Hannon¹,
Muhamad Nabil Hidayat¹, Rahimi Baharom¹, Wan Noraishah Wan Abdul Munim¹

¹School of Electrical Engineering, College of Engineering, Universiti Teknologi MARA, Shah Alam, Selangor, Malaysia

²Department of Electrical, Electronics and Systems Engineering, Universiti Kebangsaan Malaysia, Bangi, Selangor, Malaysia

Article Info

Article history:

Received Mar 12, 2024

Revised Sep 6, 2024

Accepted Sep 19, 2024

Keywords:

Adaptive linear neuron

Harmonics

Parallel resonance

Power quality

Shunt active power filter

ABSTRACT

This paper presents an adaptive linear neuron (Adaline) algorithm designed to extract resonance current from the supply current directly. It aims to reduce the computation burden while upholding efficacy in the extraction process. The approach involves establishing the primary power system, evaluating harmonic and resonance current impacts, formulating efficient extraction strategies based on current waveform characteristics, employing the Adaline algorithm for extraction, and constructing a single-phase shunt active power filter (SAPF) to address harmonic currents and parallel resonance effects. Comparative analysis demonstrates the Adaline algorithm's precision in extracting current amplitudes pre- and post-SAPF implementation. However, observed disparities in extracted resonance current amplitude may stem from the algorithm's limitations in capturing low-amplitude signals. While a gain adjustment effectively boosts amplitude. However, it introduces considerable ripple and inconsistency, likely linked to parallel resonance effects. Notably, the SAPF exhibits simultaneous harmonic compensation and resonance damping capabilities. Results affirm the SAPF's effectiveness in reducing harmonic components across all frequencies, including resonance frequency. Furthermore, resonance damping is crucial for further improving SAPF performance and reducing resonance current. This results in significantly improved waveform quality and reduced total harmonic distortion (THD) and individual harmonic distortion (THDi) values of compensated supply current.

This is an open access article under the [CC BY-SA](https://creativecommons.org/licenses/by-sa/4.0/) license.



Corresponding Author:

Nor Farahaida Abdul Rahman

School of Electrical Engineering, College of Engineering, Universiti Teknologi MARA

Shah Alam, Selangor, Malaysia

Email: farahaida@uitm.edu.my

1. INTRODUCTION

In contemporary electrical power systems, the widespread integration of capacitor banks for reactive power compensation and power factor correction has led to the emergence of resonance currents, garnering significant attention [1], [2]. These currents can have detrimental effects, causing harmonic distortion, power quality degradation, and potential equipment damage [3], [4]. Addressing resonance currents has become crucial to ensuring modern power systems' reliable and efficient operation.

Resonance currents arise due to the interaction between the capacitive reactance of the capacitor bank and the inductive reactance of the power system [5]. When the capacitive and inductive reactance are equal in magnitude but opposite in sign, a condition known as parallel resonance occurs. At this resonant frequency, the impedance of the parallel combination becomes minimal, allowing for the amplification of harmonic currents [6]. The current amplification due to resonance can lead to several adverse effects on the power system.

These include increased thermal stress on capacitor banks, transformers, and other equipment, resulting in accelerated ageing and potential failures [7]. Additionally, resonance currents can cause voltage distortion, leading to malfunctions in sensitive electronic equipment and increased losses in the system [8], [9].

In recent years, the advent of shunt active power filters (SAPFs) has emerged as a promising solution for compensating resonance currents in capacitor banks [10]-[15]. SAPFs are power electronic devices that actively inject compensating currents into the system, compensating the harmonic and resonance currents [16]. Unlike passive filters, SAPFs offer dynamic and adaptive capabilities, enabling them to respond effectively to varying system conditions and harmonic profiles [17]. The efficiency and effectiveness of SAPFs heavily rely on the extraction algorithm used to detect and analyses the harmonic currents, including resonance currents in the system.

The most common extraction algorithm used in extracting resonance currents in SAPF operation is known as the recursive discrete Fourier transform (RDFT) algorithm [11]-[13]. It is a computational algorithm that efficiently calculates the discrete Fourier transform (DFT) of a sequence of data points [18], making it suitable for analysing the frequency content of discrete-time signals [19]. The RDFT algorithm extracts the harmonic voltage component from the point of common coupling (PCC) voltage at the resonance frequency. Subsequently, the algorithm utilises the extracted harmonic voltage component to generate the resonance-damping current reference for the SAPF [11]-[13]. Figure 1(a) depicts a block diagram of a closed-loop RDFT algorithm to extract resonance current utilised in a SAPF system. Although the RDFT algorithms offer computational efficiency in Fourier transform calculations, they pose challenges regarding memory usage due to their recursive nature and the necessity to store intermediate results. This increased memory usage can be challenging, especially for large datasets or environments with limited memory resources [20].

To address the limitations of RDFT algorithms, researchers in [14] substituted them with adaptive linear neuron (Adaline) algorithms. Adaline is an artificial neural network that possesses the capability to learn and adapt to nonlinear data patterns, allowing it to effectively model intricate relationships between input and output variables [21], [22]. Additionally, it can be trained to be robust to noise and disturbances in the input data, making it suitable for applications where the data may be corrupted or noisy. Figure 1(b) shows the block diagram of the Adaline algorithm for extracting the resonance current. The authors retained the entire architecture except for the extraction algorithms.

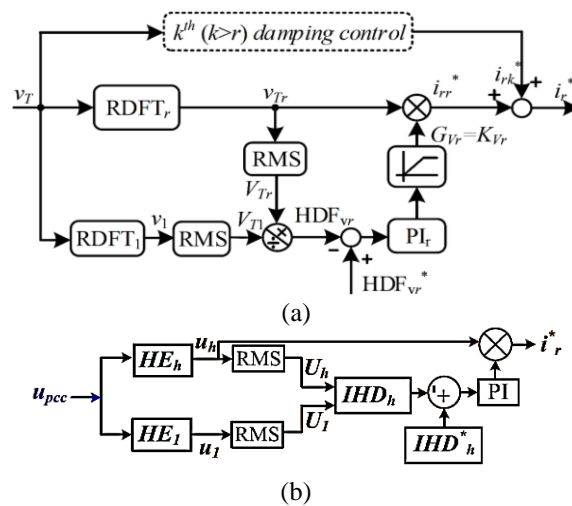


Figure 1. Extraction resonance current reference signal using (a) RDFT algorithm [8] and (b) Adaline algorithm [15]

According to Figure 1, the algorithm derived the extracted resonance current from regulating the harmonic distortion function (HDF) using a proportional-integral (PI) controller. In which the HDF was selected based on IEEE 519-1992. However, the algorithm must extract the fundamental voltage to achieve the objective. Thus, it complicates the algorithm due to the involvement of multiple parameters. Moreover, the optimal performance of both algorithms depends on precise parameter tuning in their closed-loop controllers. As a result, minor variations or inaccuracies in system parameters may result in suboptimal or unstable behavior [23]. Notably, neither extraction strategy directly extracts the resonance current from the current itself; instead, the algorithm must convert the extracted voltages to resonance current.

This research paper aims to introduce a single Adaline algorithm for extracting the resonance current. Instead of extracting the resonance current from the PCC voltage, the proposed algorithm extracts current directly from the supply current. This shift offers direct extraction strategies to alleviate the computation burden associated with traditional techniques. Furthermore, the proposed algorithm does not jeopardise the efficacy and effectiveness of the extraction process. Additionally, the paper will evaluate the performance and effectiveness of SAPFs in mitigating resonance currents, drawing comparisons with traditional techniques, and highlighting the potential benefits and challenges associated with their deployment.

2. METHODOLOGY

The methodology focuses on comprehensively analysing power system harmonics and resonance currents. Initially, the main power system is constructed, followed by an evaluation of the impact of harmonic and resonance currents. Furthermore, advanced strategies for current extraction are developed through waveform analysis, employing the Adaline algorithm, and constructing a SAPF to mitigate the effects of harmonic currents and parallel resonance.

2.1. Constructing the main power system and assessing harmonic and resonance currents impacts

Initially, two power systems are constructed. Figure 2(a) depicts a circuit configuration with an inductive nonlinear load. Meanwhile, Figure 2(b) exhibits another circuit configuration incorporating an inductive nonlinear load and a capacitor bank. Both circuits connect to a 230 V alternating current (AC) source with a small line impedance. The nonlinear load comprises a single-phase uncontrollable rectifier with an inductive element, denoted as the inductive nonlinear load. The work investigates the effects of the nonlinear load and the capacitor bank on the waveshape, total harmonic distortion (THD) and individual harmonic distortion or distortion factor (THDi) of the instantaneous supply current waveform. The THDi values are compared with the IEEE 519-2014 standard. Subsequently, the relationship between the system's instantaneous currents is studied to ascertain the appropriate strategy to extract the resonance current.

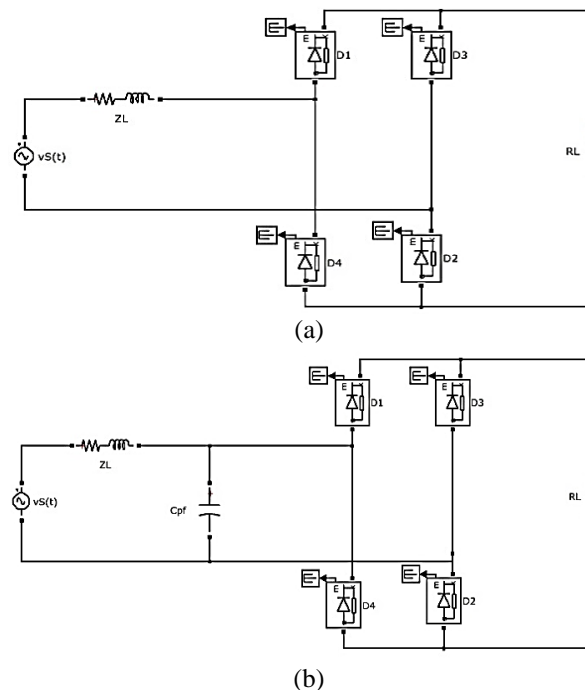


Figure 2. Circuit configuration consists of (a) nonlinear load only and (b) nonlinear load and capacitor bank

2.2. Assessing the properties of current waveforms to develop effective strategies for current extraction

Understanding the properties of current waveforms before and after the SAPF implementation is crucial for devising effective strategies in the resonance current extraction technique. Figure 3 shows the flow

of all currents within the power system before and after the SAPF implementation. According to Figure 3(a), the instantaneous supply current $i_s(t)$ equals the instantaneous load current $i_L(t)$. Thus, as in (1).

$$i_s(t) = i_L(t) \quad (1)$$

However, due to the nonlinearity of the load and the parallel resonance stemming from the capacitor bank C_{PF} , $i_L(t)$ encompasses fundamental, resonance, and harmonic load current components. It can be expressed as (2) and (3). Where:

$i_{L1}(t)$ is the instantaneous fundamental load current with an amplitude of I_{L1} .

$i_{Lr}(t)$ is the instantaneous resonance load current with an amplitude of I_{Lr} .

$i_{Lh}(t)$ is the instantaneous harmonic load current with an amplitude of I_{Lh} .

$$i_L(t) = i_{L1}(t) + i_{Lr}(t) + \sum_{h=3,7,9,\dots}^{\infty} i_{Lh}(t) \quad (2)$$

$$i_L(t) = I_{L1} \sin(\omega t) + I_{Lr} \sin(\omega t - \theta_r) + \sum_{h=3,7,9,\dots}^{\infty} I_{Lh} \sin(\omega t - \theta_h) \quad (3)$$

By replacing (3) with (1), found (4).

$$i_s(t) = I_{L1} \sin(\omega t) + I_{Lr} \sin(\omega t + \theta_r) + \sum_{h=3,7,9,\dots}^{\infty} I_{Lh} \sin(\omega t + \theta_h) \quad (4)$$

According to Figure 3(b), (4) becomes (5).

$$i_s(t) + i_F(t) = I_{L1} \sin(\omega t) + I_{Lr} \sin(\omega t + \theta_r) + \sum_{h=3,7,9,\dots}^{\infty} I_{Lh} \sin(\omega t + \theta_h) \quad (5)$$

Where $i_F(t)$ is the instantaneous compensation current injected by the SAPF.

When the SAPF solely performs harmonic compensation, $i_F(t)$ properties include resonance and harmonic components. It can be expressed as (6).

$$i_F(t) = I_{Lr} \sin(\omega t + \theta_r) + \sum_{h=3,7,9,\dots}^{\infty} I_{Lh} \sin(\omega t + \theta_h) \quad (6)$$

Nevertheless, as outlined in [13], residual harmonic currents can still trigger parallel resonance, distorting the supply current around the resonance frequency. Consequently, as in (7). I_{Sr} is the amplitude of the resonance current due to the interaction between the residual harmonic currents and CPF.

$$i_s(t) = I_{L1} \sin(\omega t) + I_{Sr} \sin(\omega t + \theta_r) \quad (7)$$

Thus, SAPF must also extract the residual resonance current to enhance resonance damping. According to (7), it is feasible to extract the residual resonance current from the $i_s(t)$ waveform instead of the $i_L(t)$ waveform, as practiced by other researchers. This work extracts the residual resonance current using a single adaptive linear neuron (Adaline) algorithm to simplify the extraction process.

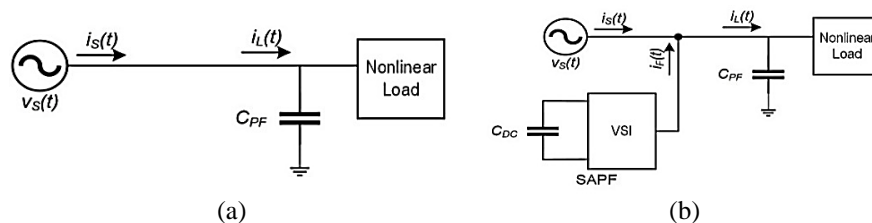


Figure 3. Current flows: (a) before and (b) after SAPF implementation

2.3. Utilising Adaline algorithm to extract fundamental load current and residual resonance supply current components

Figure 4 shows the configuration of the Adaline algorithms designed to extract the I_{L1} and resonance current I_{Sr} components. The figure shows that the resonance current extraction only requires a single algorithm for the extraction process. Hence, simplify the computational process of extracting the component. Both

algorithms use the same operating principle to derive the amplitude of both components. Detailed insights into the execution of the extraction process by the Adaline algorithms are provided in [24], [25].

As per the depiction in Figure 4, the $i_{Lh}(t)$ signal is generated by computing the difference between the extracted $i_{Ll}(t)$ with the measure $i_L(t)$. Subsequently, the combination of the resultant $i_{Lh}(t)$ and the extracted $i_{Sr}(t)$ yields the instantaneous reference signal $i_{ref}(t)$ utilised for the SAPF. The filter integrates a hysteresis controller to regulate $i_F(t)$ by generating a pulse width modulation (PWM) signal for the filter's operation. The extracted signals are compared with the same parameters generated by the MATLAB fast Fourier transform (FFT) analysis to verify the Adaline algorithm's efficacy.

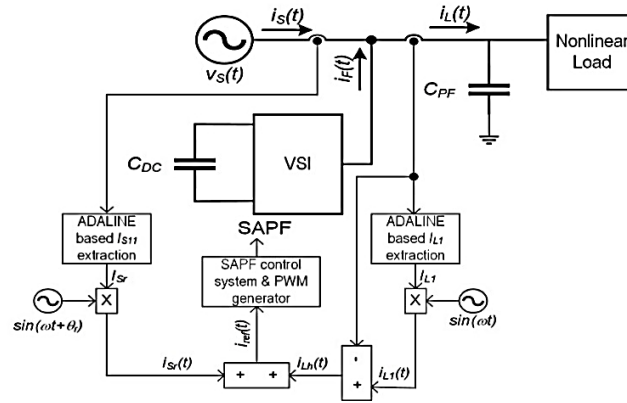


Figure 4. Adaline configuration for extracting I_{Ll} and I_{Sr} signals

2.4. Constructing SAPF and exploring the effects of harmonic currents and parallel resonance

According to Figure 3(b) until Figure 4, the work implements a single-phase voltage source inverter (VSI) as a SAPF. The inverter exhibits a conventional four-switch configuration with a direct current (DC)-link capacitor, C_{DC} . The DC-link voltage is set at 650 V to ensure the SAPF can inject sufficient $i_F(t)$ into the main power system. Subsequently, investigating the effects of harmonic current and parallel resonance on the quality of the $i_S(t)$ waveform entails observation, measurement, and comparison. This examination is particularly critical when the SAPF performs two distinct functions: harmonic current compensation and resonance current damping.

3. RESULTS AND DISCUSSION

Figure 5 illustrates the impact of parallel resonance on current waveforms in a power system with a nonlinear load. In Figure 5(a), distortions in the current waveform are visible due to harmonic currents generated by the nonlinear load, with a THD value of 11.89%. However, Figure 5(b) demonstrates a notably more distorted current waveform than Figure 5(a). The increased distortion is attributed to the introduction of resonance current caused by the capacitor bank. The THD spikes significantly to 88.66%. The graphs demonstrate that parallel resonance can greatly intensify current distortion in a power system with a nonlinear load. Furthermore, it also shows that the parallel resonance occurs in the 11th harmonic order, 550 Hz.

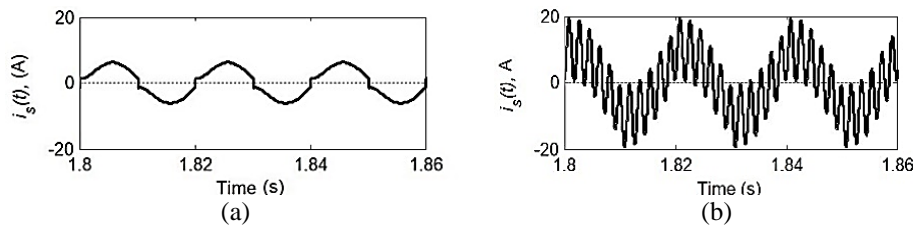
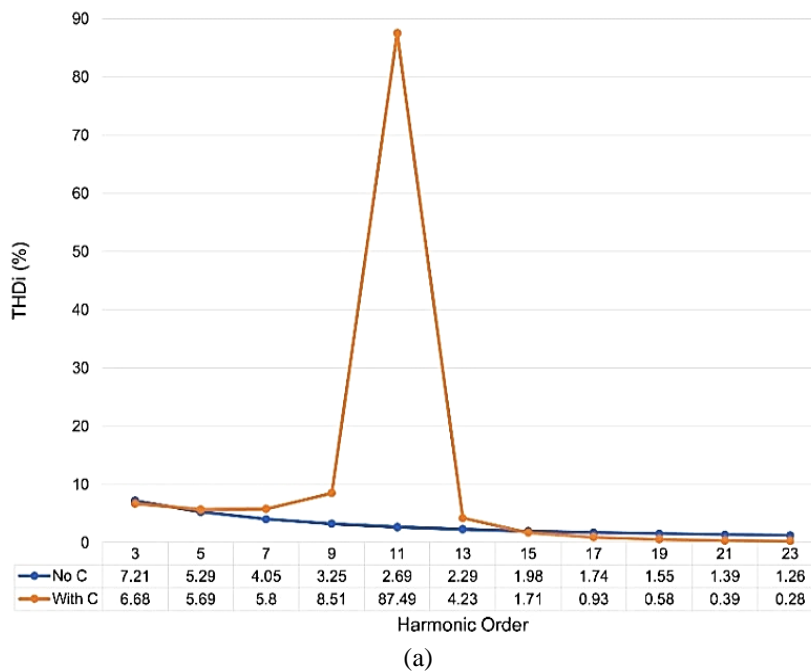


Figure 5. Waveforms of $i_S(t)$: (a) without and (b) with parallel resonance effect

Figure 6(a) presents the impact of parallel resonance on the current waveform's THDi values. Concurrently, Figure 6(b) shows a tabulated breakdown of individual distortion limits according to the IEEE

519-2014 standard. Without parallel resonance, THDi values across various harmonic orders range from 1.26% to 7.21%, surpassing the permissible limit of 0.38%. These percentages indicate a current waveform closer to a pure sine wave, suggesting moderate distortion solely due to the nonlinear load. However, with parallel resonance, THD values dramatically escalate from 0.28% to an alarming 87.49%. The high THDi percentages indicate that the parallel resonance amplifies distortion, particularly around the 9th and 11th harmonic components. However, Figure 6(a) shows that the capacitor bank can mitigate THD values at higher harmonic orders than the resonance frequency, approaching the IEEE limits. Nevertheless, the effect is overshadowed by the dominance of THDi values near the resonance frequency. In summary, Figure 6(a) demonstrates that parallel resonance significantly increases the THDi of individual harmonic components in a power system, potentially breaching IEEE Standard 519-2014.

Figure 7 shows the extraction signals of $i_{LI}(t)$ and $i_{SII}(t)$ to validate the effectiveness of the Adaline algorithm. As mentioned, the $i_{LI}(t)$ and $i_{SII}(t)$ signals were extracted from $i_L(t)$ and $i_S(t)$ waveforms, respectively. When comparing Figure 7(a) with the current amplitudes obtained from the MATLAB FFT analysis, the Adaline algorithm accurately extracts current amplitudes of 10 A and 8.76 A before implementing SAPF. However, with the SAPF in operation, the Adaline extracts a lower $i_{SII}(t)$ signal from the compensated $i_S(t)$ waveform, as shown in Figure 7(b). According to the MATLAB FFT analysis, the Adaline should extract a signal of 0.22 A of resonance current. However, Figure 7(b) exhibits a lower amplitude of the $i_{SII}(t)$ signal extracted by the Adaline algorithm. The discrepancy may result from the Adaline algorithm's limitation in extracting low-amplitude signals when the SAPF operation introduces a nonlinear relationship between its input and output signals [26]. Nevertheless, introducing a gain of 1.4 has effectively increased the amplitude of the extracted $i_{SII}(t)$ signal. Besides that, the extracted $i_{SII}(t)$ signal consists of a high ripple and inconsistency. It may cause by the parallel resonance. These findings underscore both the functionality and the challenges of the Adaline algorithm in signal extraction processes.



I_{SC}/I_L	Individual harmonic limits (Odd harmonics) ^{a,b} Harmonics values are in % of maximum demand load current					TDD
	$3 \leq h < 11$	$11 \leq h < 17$	$17 \leq h < 23$	$23 \leq h < 35$	$35 \leq h \leq 50$	
<25°	1.0	0.5	0.38	0.15	0.1	1.5
20<50	2.0	1.0	0.75	0.3	0.15	2.5
≥50	3.0	1.5	1.15	0.45	0.22	3.75

(b)

Figure 6. Individual THD value of (a) $i_S(t)$ waveform without (orange) and with (blue) parallel resonance and (b) IEEE 519-2014 standard

Figure 8 presents waveforms of $i_S(t)$, $i_F(t)$, and $i_L(t)$ under two conditions: harmonic compensation only, show in Figure 8(a) and harmonic compensation with resonance damping, show in Figure 8(b). Meanwhile, Figure 9 illustrates THDi values for these scenarios. The waveshape of both $i_S(t)$ waveforms reveals that the SAPF can separately or concurrently perform harmonic compensation and resonance damping functions. However, Figure 8(a) exhibits more pronounced distortion in $i_S(t)$ waveform than Figure 8(b). It is evident that the peaks and troughs are more irregular in Figure 8(a) compared to the smoother waveform in Figure 8(b). The THD values for Figures 8(a) and 8(b) are 4.01% and 3.49%, respectively. Despite the roughness of the $i_S(t)$ waveform in Figure 8(a), the finding in Figure 9 demonstrates that the harmonic compensation function effectively minimizes all harmonic components at all frequencies, including the resonance frequency.

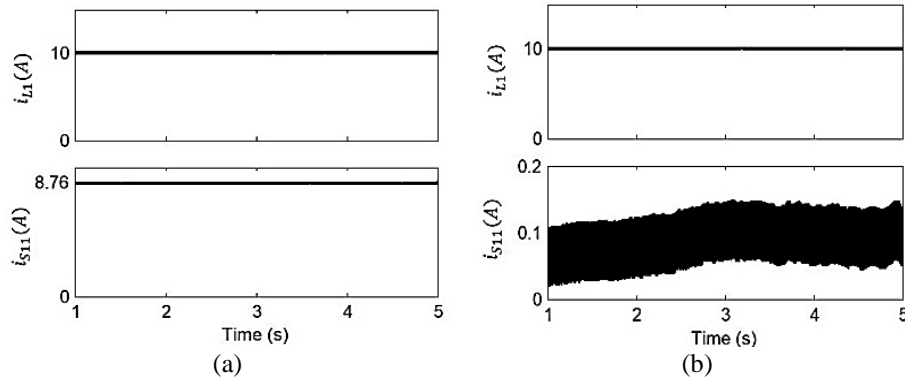


Figure 7. Extraction signals of $i_S(t)$ and $i_{S11}(t)$ by Adaline: (a) before and (b) after the SAPF implementation

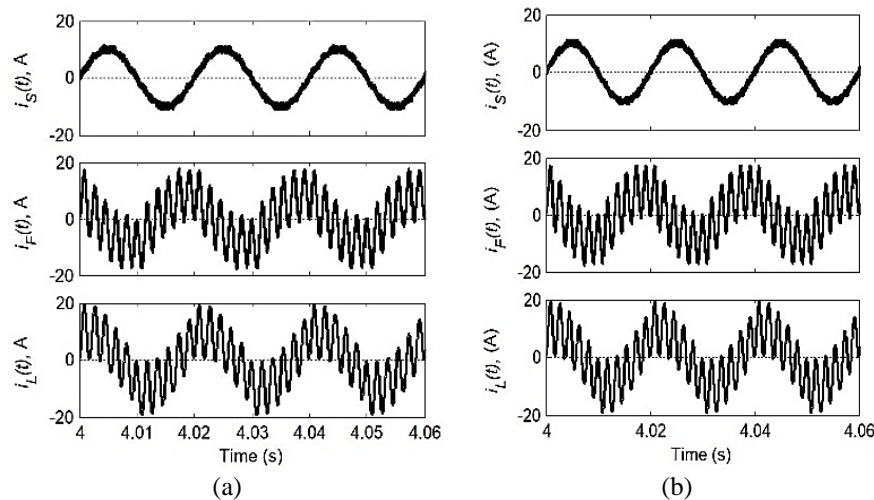


Figure 8. Waveforms of $i_S(t)$, $i_F(t)$ and $i_L(t)$ when the SAPF performs: (a) harmonic compensation only and (b) harmonic compensation and resonance damping

According to Figures 6(a) and 9, the individual THDi of the resonance current reduced from 87.49% to 2.19%. However, this improvement is insufficient compared to the individual THDi without the parallel resonance effect, as shown in Figure 6(a). Therefore, the resonance damping function is crucial to enhance SAPF performance further and reduce the resonance current. According to Figure 9, resonance damping reduces the THDi of the resonance current from 2.19% to 0.99%. Therefore, introducing the resonance damping function improves the waveform quality significantly, resulting in a smoother and less distorted source current. Moreover, resonance damping substantially reduces the THD and THDi values caused by the resonance current.

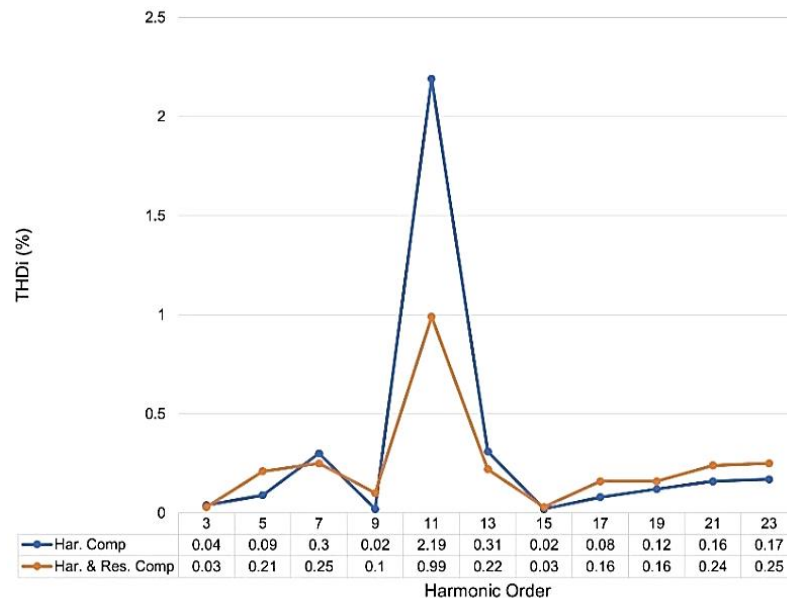


Figure 9. THDi value of $i_s(t)$ waveform when SAPF performing harmonic compensation only (blue) and with both harmonic compensation and resonance damping (orange)

4. CONCLUSION

All results have successfully verified the objective. The findings show that the parallel resonance at 550 Hz shoots up the $i_s(t)$'s THD values by 745.67% due to the increase in THDi value at 550 Hz by 3252.42%. Nevertheless, the simple and direct extraction algorithm and strategy demonstrated the SAPF's capacity to address harmonic and resonance currents effectively. According to the findings, the SAPF can reduce the $i_s(t)$'s THD value to 4.01% with harmonic compensation only and 3.49% with harmonic and resonance damping functions. Moreover, the results offer valuable insights into the SAPF's potential to mitigate resonance currents even without a damping function. However, the damping function is essential to enhance the SAPF performance, especially for resonance damping. Using the proposed extraction algorithm and strategy, the SAPF can compensate and damp harmonic and resonance currents to ensure the THD and THDi values of $i_s(t)$ adhere to the stringent criteria outlined in the IEEE 519-2014 standard.




REFERENCES

- [1] A. Luo, S. Peng, C. Wu, J. Wu and Z. Shuai, "Power electronic hybrid system for load balancing compensation and frequency-selective harmonic suppression," *IEEE Transactions on Industrial Electronics*, vol. 59, no. 2, pp. 723-732, Feb. 2012, doi: 10.1109/TIE.2011.2161066.
- [2] Y. Xie, H. Yi, F. Zhuo, Y. Li, X. Jiang, and Z. Zhang, "Analysis and stabilization for full harmonic compensation oscillation in SAPF system with source current direct control," *IET Power Electronics*, vol. 17, no. 1, pp. 107–120, Dec. 2023, doi: 10.1049/pel2.12619.
- [3] D. Tong, V. G. Nikolaenko, N. Ginbey and I. Lau, "Harmonic propagation in transmission system with multiple capacitor installations," in *Proceeding of 2000 International Conference on Power System Technology*, Perth, WA, Australia, 2000, pp. 1007-1012 vol.2, doi: 10.1109/ICPST.2000.897158.
- [4] Ł. Michalec, M. Jasiński, T. Sikorski, Z. Leonowicz, Ł. Jasiński, and V. Suresh, "Impact of harmonic currents of nonlinear loads on power quality of a low voltage Network—Review and Case Study," *Energies*, vol. 14, no. 12, p. 3665, Jun. 2021, doi: 10.3390/en14123665.
- [5] J. C. Das, *Power System Harmonics and Passive Filter Designs*. New Jersey: Wiley, Mar. 06, 2015. doi: 10.1002/9781118887059.
- [6] S. Rahmani, K. Al-Haddad and F. Fnaiech, "A three-phase shunt active power filter for damping of harmonic propagation in power distribution systems," in *Proceeding of 2006 IEEE International Symposium on Industrial Electronics*, Montreal, QC, Canada, 2006, pp. 1760-1764, doi: 10.1109/ISIE.2006.295837.
- [7] R. János and D. Pitićă, "Accelerated ageing tests for predicting capacitor lifetimes," in *Proceeding of 2011 IEEE 17th International Symposium for Design and Technology in Electronic Packaging (SIITME)*, Timisoara, Romania, 2011, pp. 63-68, doi: 10.1109/SIITME.2011.6102687.
- [8] S. R. Mohamed, M. Alarfaj, M. H. Shwehdi, A. Bubshait and A. Smadi, "Investigation of harmonics and transient over voltages due to capacitor bank switching on distribution network," *International Journal of Advanced Science and Technology*, vol. 29, no. 10s, pp. 7947-7957, 2020.
- [9] A. L. Motalub and E. Iheanyichukwu, "Effects of capacitor bank installation in a medium voltage (MV) substation," *Innovative Systems Design and Engineering*, vol.8, no.3, pp. 19-24, 2017.
- [10] S. Khalid, "A novel Algorithm Adaptive Autarchoglossans Lizard Foraging (AALF) in a shunt active power filter connected to MPPT-based photovoltaic array," *e-Prime - Advances in Electrical Engineering, Electronics and Energy*, vol. 3. p. 100100, Mar. 2023. doi: 10.1016/j.prime.2022.100100.




- [11] Y. Zhang, K. Dai, X. Chen, Y. Kang and Z. Dai, "An improved method of SAPF for harmonic compensation and resonance damping with current detection of power capacitors and linear/nonlinear loads," in *Proceeding of 2017 IEEE Applied Power Electronics Conference and Exposition (APEC)*, Tampa, FL, USA, 2017, pp. 3286-3291, doi: 10.1109/APEC.2017.7931168.
- [12] C. Liu, Y. He, K. Dai and Y. Kang, "Industrial power distribution system harmonic resonance problem and solution with shunt active power filter," in *Proceeding of IECON 2017 - 43rd Annual Conference of the IEEE Industrial Electronics Society*, Beijing, China, 2017, pp. 1243-1248, doi: 10.1109/IECON.2017.8216212.
- [13] X. Chen, K. Dai, C. Xu, L. Peng, and Y. Zhang, "Harmonic compensation and resonance damping for SAPF with selective closed-loop regulation of terminal voltage," *IET Power Electronics*, vol. 10, no. 6, pp. 619–629, May 2017. doi: 10.1049/iet-pel.2016.0344.
- [14] S. Sharma, V. Verma, M. Tariq and S. Urooj, "Reduced sensor-based harmonic resonance detection and its compensation in power distribution system with SAPF," *IEEE Access*, vol. 10, pp. 59942-59958, 2022, doi: 10.1109/ACCESS.2022.3176366.
- [15] A. Saim, A. Houari, M. Ait-Ahmed, M. Machmoum, and J. M. Guerrero, "Active resonance damping and harmonics compensation in distributed generation based islanded microgrids," *Electric Power Systems Research*, vol. 191, p. 106900, Feb. 2021. doi: 10.1016/j.epsr.2020.106900.
- [16] K. Kalyan, M. S. Rao and S. Gawre, "Improvement of power quality using series active power filter (SAPF)," in *Proceeding of 2020 IEEE International Students' Conference on Electrical, Electronics and Computer Science (SCEECS)*, Bhopal, India, 2020, pp. 1-5, doi: 10.1109/SCEECS48394.2020.151.
- [17] J. Yang and Y. Ding, "A novel starting impulse suppression method for active power filter based on slowly rising curve," *Energy Engineering*, vol. 118, no. 6, pp. 1839–1853, 2021. doi: 10.32604/ee.2021.015930.
- [18] C. Xu, K. Dai, X. Chen, L. Peng, Y. Zhang and Z. Dai, "Parallel resonance detection and selective compensation control for sapf with square-wave current active injection," *IEEE Transactions on Industrial Electronics*, vol. 64, no. 10, pp. 8066-8078, Oct. 2017, doi: 10.1109/TIE.2017.2696461.
- [19] MD Analysis, "Radial distribution functions," [Online] Available: https://docs.mdanalysis.org/1.1.0/documentation_pages/analysis/rdf.html. [Accessed: Mar. 8, 2024].
- [20] DS-Client, "Memory requirements for DS-Client during incremental backup using delta algorithm," 2009. [Online] Available: https://s3.amazonaws.com/asigra-documentation/Help/DS-Client%20Help/index.html#page/DS-Client_Help/Memory_Requirements_for_DS-Client_During_Increme.html. [Accessed: Mar. 8, 2024].
- [21] A. N. Handayani, A. D. Aindra, D. F. Wahyulis, S. Pathmantara, and R. A. Asmara, "Application of Adaline artificial neural network for classroom determination in elementary school," *IOP Conference Series: Materials Science and Engineering*, vol. 434, p. 012030, Dec. 04, 2018. doi: 10.1088/1757-899x/434/1/012030.
- [22] C. L. C. Mattos, J. D. A. Santos, and G. A. Barreto, "Improved Adaline networks for robust pattern classification," in *Proceeding of Artificial Neural Networks and Machine Learning – ICANN 2014*, 2014, pp. 579–586, doi: 10.1007/978-3-319-11179-7_73.
- [23] GE Digital, "Overview of control loop tuning," 2023. [Online] Available: https://www.ge.com/digital/documentation/csense/version85/Continuous%20Wizard/Introduction_to_Loop_Tuning.htm. [Accessed: Mar. 8, 2024].
- [24] K. Hasan *et al.*, "Online harmonic extraction and synchronisation algorithm based control for unified power quality conditioner for microgrid systems," *Energy Reports*, vol. 8, pp. 962–971, Apr. 2022. doi: 10.1016/j.egyr.2021.11.002.
- [25] M. Qasim, P. Kanjiya and V. Khadkikar, "Optimal current harmonic extractor based on unified ADALINEs for shunt active power filters," *IEEE Transactions on Power Electronics*, vol. 29, no. 12, pp. 6383-6393, Dec. 2014, doi: 10.1109/TPEL.2014.2302539.
- [26] D.-J. Jwo, A. Biswal, and I. A. Mir, "Artificial neural networks for navigation systems: A review of recent research," *Applied Sciences*, vol. 13, no. 7, p. 4475, Mar. 31, 2023. doi: 10.3390/app13074475.

BIOGRAPHIES OF AUTHORS






Nor Farahaida Abdul Rahman    works as a senior lecturer at the School of Electrical Engineering, College of Engineering, Universiti Teknologi MARA, Shah Alam, Selangor, Malaysia. She received her B.Eng. (Hons.) and M.Eng. degrees from Universiti Teknologi Malaysia (UTM), and Ph.D. in Power Engineering from Universiti Putra Malaysia (UPM). Her research interests are active filters, power quality and power electronics. She can be contacted at email: farahaida@uitm.edu.my.






Muhammad Ammirul Atiqi Mohd Zainuri    received the B.Eng. in Electrical and Electronic Engineering from Universiti Putra Malaysia, in 2011, the M.Sc. of Electrical Power Engineering from Universiti Putra Malaysia, in 2013, and In August 2017, he was awarded his Ph.D. degree from Department of Electrical and Electronic Engineering, Faculty of Engineering, Universiti Putra Malaysia. He is a member of IEEE and a registered graduate engineers Malaysia (BEM) in the electrical track. Currently, he is a senior lecturer at Department of Electrical, Electronic and System Engineering, Universiti Kebangsaan Malaysia (UKM). He has authored and co-authored number of well recognised journals and conference papers. His research interests are in power electronics, power quality, renewable energy systems and applied artificial intelligent in electrical systems. He is an active research member at UMPEDAC and ALPER (UPM). He can be contacted at email: ammirulatiqi@ukm.edu.my.






Naeem M. S. Hannon    is an accomplished professional with diverse experience in the field of electrical engineering. He spent four years at a thermal power plant in Kuwait, focusing on maintenance, troubleshooting, and scheduling for generators, motors, and transformers. In Malaysia, he served as a site engineer for two years, contributing to the design and commissioning of substations. As an associate professor, he has provided consultation and technical training to various power industries globally, including in Dubai and London. Currently, he works as a technical consultant for both government and private sectors, alongside his role at the School of Electrical Engineering, College of Engineering, Universiti Teknologi MARA. He has authored numerous technical articles and received grants for his research in power generation stability, protection, and AI-control of power systems. He can be contacted at email: naeem@uitm.edu.my.






Muhamad Nabil Hidayat    is an expert in energy audit assessment, renewable energy management and well adopted in Japanese working culture and aspiration. He is currently held a position as head of Battery Energy Storage Technology Laboratory at MNA Facility in Universiti Teknologi MARA Shah Alam, Selangor. He has done energy efficiency projects locally and international for the past 10 years. Prominent projects are the rural electrification project in Sabah Malaysia, energy efficient projects under RMK-11 with SEDA and GREENTECH Malaysia, and sustainable renewable energy project with Toyama Prefecture, Japan. He can be contacted at email: mnabil@uitm.edu.my.



Rahimi Baharom    is a lecturer in School of Electrical Engineering, College of Engineering, Universiti Teknologi MARA, Malaysia since 2009; and he has been a senior lecturer since 2014. He received the B.Eng. degree in Electrical Engineering and the M.Eng. degree in Power Electronics, both from Universiti Teknologi MARA, Malaysia, in 2003 and 2008, respectively; and Ph.D. degree in Power Electronics also from Universiti Teknologi MARA, Malaysia in 2018. He is a senior member of IEEE and also a corporate member of the Board of Engineers Malaysia and the member of Malaysia Board of Technologists. His research interests include the field of power electronics, motor drives, industrial applications, and industrial electronics. He can be contacted at email: rahimi6579@uitm.edu.my.



Wan Noraishah Wan Abdul Munim    received the diploma in Electrical Engineering (communication) from University Teknologi Malaysia, Skudai, Malaysia, in 2003, the B.Eng. Technology degree in Electrical Engineering from Universiti Kuala Lumpur, Kuala Lumpur, Malaysia, in 2007, the M.Sc. degree in Electrical Power Engineering with business from the University of Strathclyde, Glasgow, U.K., in 2009 and the Ph.D. degree in Electrical Engineering at UM Power Energy Dedicated Advanced Centre, University of Malaya, Kuala Lumpur, Malaysia, in 2020. She is a lecturer in School of Electrical Engineering, College of Engineering, Universiti Teknologi MARA, Shah Alam, Malaysia since 2010; and she has been a senior lecturer since 2017. Her research interests include multiphase machines and drives, fault-tolerant control, and renewable energy. She received the 2014 Ministry of Education Malaysia Skim Latihan Akademik IPTA (SLAI) Scholarship Award for her Ph.D. study. She can be contacted at email: aishahmunim@uitm.edu.my.